Optical Coherence Tomography detection of shear wave propagation in layered tissue equivalent phantoms

Marjan Razani[1], Adrian Mariampillai[2] ,Peter Siegler[2] ,Victor X.D. Yang[2,3], Michael C. Kolios[1,*]

(1) Department of Physics, Ryerson University, Toronto, Canada
(2) Department of Electrical and Computer Engineering, Ryerson University, Toronto, Canada
(3) Division of Neurosurgery, University of Toronto, Toronto, Canada
*mkolios@ryerson.ca

Abstract

In this work, we explored the potential of measuring shear wave propagation using Optical Coherence Elastography (OCE) in a layered phantom and based on a swept-source optical coherence tomography (OCT) system. Shear waves were generated using a piezoelectric transducer transmitting sine-wave bursts of 400 μs, synchronized with an OCT swept source wavelength sweep imaging system. The acoustic radiation force was applied to layered phantoms. The phantoms were composed of gelatin and titanium dioxide. Differential OCT phase maps, measured with and without the acoustic radiation force, demonstrate microscopic displacement generated by shear wave propagation in these phantoms of different stiffness. The OCT phase maps are acquired with a swept-source OCT (SS-OCT) system. We present a technique for calculating tissue mechanical properties by propagating shear waves in inhomogeneous tissue equivalent phantoms using the Acoustic Radiation Force (ARF) of an ultrasound transducer, and measuring the shear wave speed and its associated properties in the different layers with OCT phase maps. This method lays the foundation for future studies of mechanical property measurements of heterogeneous tissue structures, with applications in the study of aneurysms and other intravascular pathologies.

Keywords: Shear wave, Elastography, Optical Coherence Elastography, Acoustic Radiation Force (ARF), mechanical properties, inhomogeneous tissue equivalent phantoms.

1. Introduction

Elastography is a method in which stiffness or strain images of biomaterials are generated to characterize the biomaterial biomechanical properties [1]. An imaging modality is used to image the biomaterial deformation behavior under a static or dynamic load and generate images called elastograms. Elastograms contain information about local variations of the stiffness inside a region of interest and may provide information to aid in the identification of biomaterial defects. The shear modulus of biomaterials in particular is thought to be highly sensitive to variations in biomaterial properties.

Photonic Therapeutics and Diagnostics IX, edited by Nikiforos Kollias, et al., Proc. of SPIE Vol. 8565, 85654Q · © 2013 SPIE · CCC code: 1605-7422/13/$18 · doi: 10.1117/12.2005607

Different imaging modalities can be used to measure displacements and estimate the resulting mechanical properties such as ultrasound or magnetic resonance imaging (MRI) [2]. The main drawbacks of MRI are that it is technologically complex and expensive. Moreover, both MRI and ultrasound do not have sufficient resolution to detect small scale and subtle elastic variations in biomaterials and tissues (such as in tissue engineered modules and atherosclerotic plaques). Optical Coherence Tomography (OCT) is an optical tomographic imaging technique that shares many similarities to ultrasound despite using light. OCT has several advantages over other imaging modalities, primarily due to its inherently high resolution and motion sensitivity, which allows for the identification of micron sized morphological tissue structures and highly localized strains [3-5]. The technology is also flexible and inexpensive.

When the acoustic radiation force (ARF) is applied to a given spatial volume for a short time duration, shear waves are generated that propagate away from the initial region of excitation (i.e. the focal spot region) [6]. Shear-wave propagation speed and attenuation are directly related to the mechanical properties of the tissue. Typical values for the speed of shear waves in tissue are of the order of a 1-10 m/s, and the attenuation coefficient of soft tissues are two or three orders of magnitude greater than that of compressional waves. Due to the high attenuation of shear waves, the shear wave is generated only within a very limited area of tissue [6]. The frequency content of the shear wave will be determined primarily by the width of the ultrasound beam and not the time duration of the excitation, unless the excitation duration approaches the natural time constants of soft tissues. Therefore, smaller ultrasound beams will generally produce higher frequency shear waves in tissues.

2. Method and materials

Optical Coherence Tomography (OCT) provides imaging with histological resolution, which allows for the identification of micron sized tissue structures. Optical coherence elastography (OCE) measures tissue displacement using OCT and benefits from the high resolution of OCT to generate high-resolution stiffness maps. In this work, we explore the potential of measuring shear wave propagation in layered phantoms using OCT as an imaging modality to detect the shear wave propagation.

To achieve this, the acoustic radiation force produced by focused ultrasound beams was used to produce the shear waves. The ARF (internal mechanical excitation) was applied using a 20 MHz, circular, piezoelectric transducer element (PZT, the full width at half maximum was calculated to be 246 μm) transmitting sine-wave bursts of 400 μs. The internal displacements induced by the shear waves were detected using optical coherence tomography and phase sensitive motion algorithms. A Thorlabs SS-OCT system was used in this study. The laser had a center wavelength of a 1310 nm, a bandwidth of ~110 nm, and an A-scan rate of 8 kHz. The lateral resolution was approximately 13 μm in the samples. Using this technique, mechanical properties of the phantoms can be measured.

The phantom in this study consisted of gelatin mixed with titanium dioxide as a scattering agent. Different gelatin concentrations were used to achieve layers with different stiffnesses values. Gelatin powder (Type B, Fisher Scientific, G7-500) and distilled water were heated in a water bath at 60−65 ^{0}C for one hour and periodically stirred. Two tissue phantoms with different gelatin concentrations were prepared. When the phantom samples cooled to 45 ^{0}C, 0.1% weight by weight titanium dioxide oxide nanopowder (Sigma-Aldrich, Titanium(IV), <25 nm particle size (99.7% trace metals) was added and thoroughly mixed. The phantom solution was poured into rectangle molds (20 mm height) and allowed to congeal, however to make a second layer we left one layer to cool down and when added the second on top as shown in Figure 1.

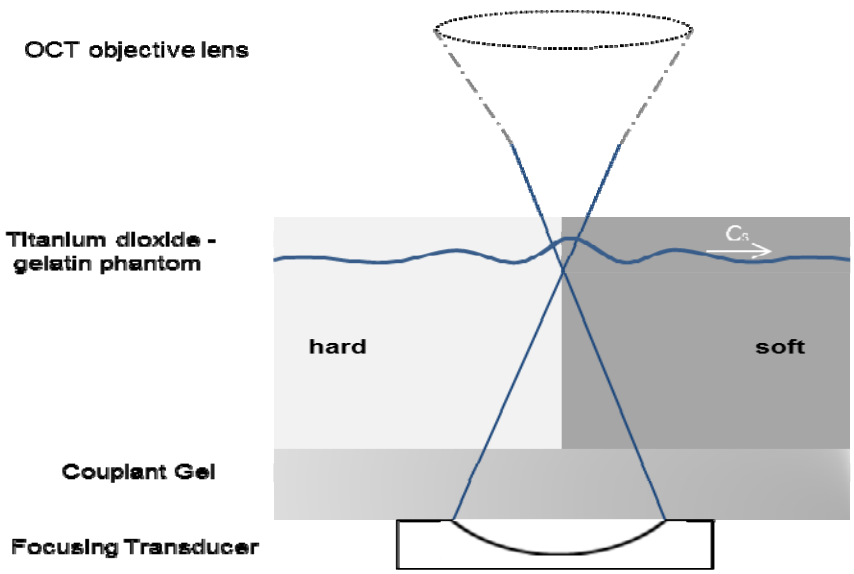

Fig. 1. A focused transducer was used to produce an ARF impulse to generate shear waves at the focal point of the transducer. The shear wave propagated in the phantom the consisted of two layers that were labeled as hard and soft, with the hard layer having two times greater gelatin concentration than the soft layer.

We used the same experimental set-up used in our previous work [7].

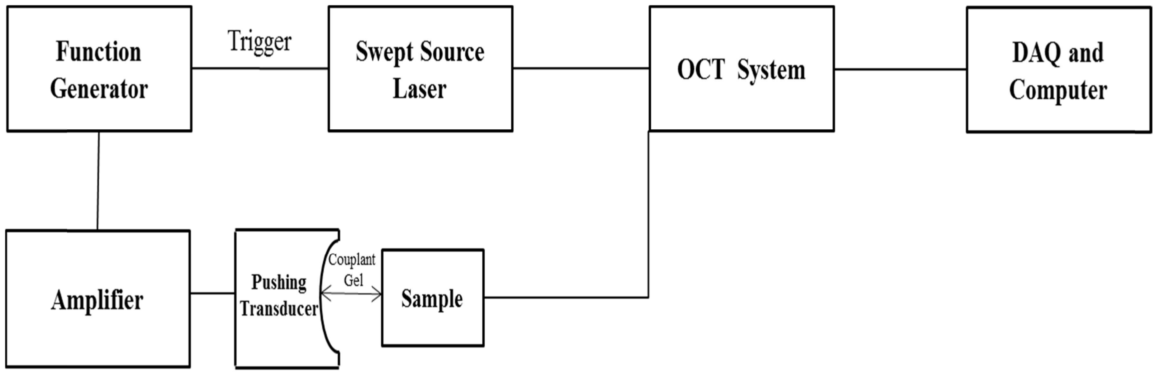

Fig. 2. A schematic diagram of the ARF-OCE experimental setup. The setup consisted of the existing SS-OCT system, a layered titanium dioxide-gelatin phantom, a focused transducer (20 MHz, f-number 2.35), an amplifier and a function generator (Agilent 33250A 80 MHz, Function / Arbitrary Waveform Generator) synchronized with the SS-OCT system.

Image intensity along a profile through the ultrasound focus was plotted for different phase offsets between the mechanical excitation and the OCT (from 0 to 2π). The image intensity profiles of all phase offsets were composed in one diagram to provide a visual aid in estimating the attenuation of the mechanical wave amplitude. The attenuation of the shear wave as it propagates through the phantom is given by the equation 1:

$$I = I_0 \exp(-\alpha x) \quad (1)$$

Where I is the intensity of the shear wave that has propagated a distance x through the material, I_0 is the initial intensity of the shear wave and α is the shear wave attenuation coefficient.

3. Results

OCT images of the layered phantoms were taken with the SS-OCT system and B- mode phase maps were obtained. These data provide information that is required to calculate the distance between two measurement points and the phase shift between these two locations for each layer. These parameters (Δr and $\Delta\varphi$) are required to calculate the shear wave speed. As described in more detail in previous work [7], using Δr and $\Delta\varphi$ we calculated the shear modulus and Young modulus.

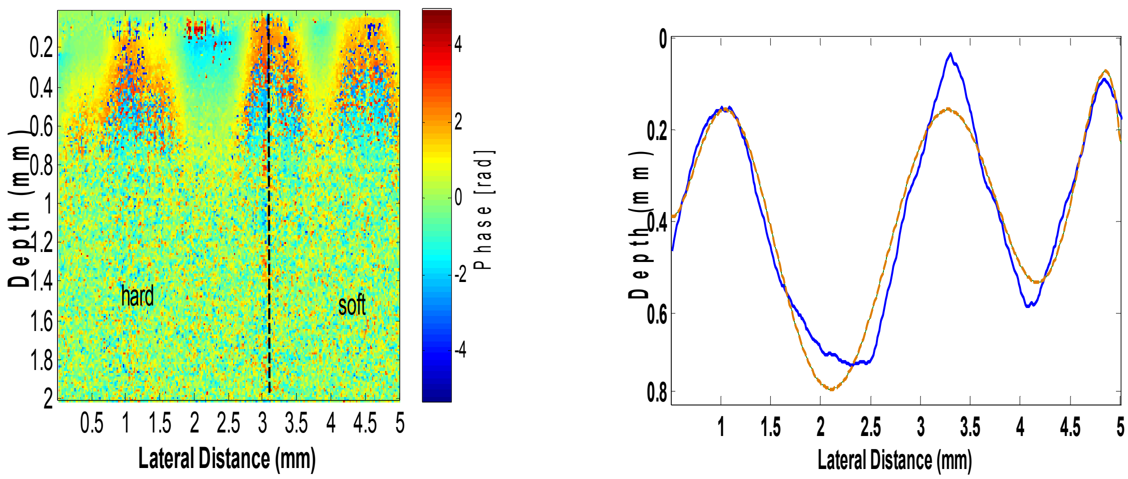

(a) (b)

Fig. 3. (a) The B-mode phase map of the phantom was used to measure Δr and $\Delta\varphi$ for the calculation of the shear wave speed. The color scale represents the change of the phase value (radians). The two layers (labeled with the arrows) had different gelatin concentrations. **(b)** To better illustrate the calculation of Δr , the experimental data (blue) were curve fitted by a polynomial (red line) to create an isophase presentation of the image in (a),

The optical path displacement z is calculated from the measured phase as $z = \lambda_0\Delta\phi/4\pi n$ [8] where λ_0 is the center wavelength of the OCT beam and n is the sample refractive index. In this figure 2 the x-axis is lateral distance within the phantom and y axis is depth. The color represents the displacement calculated from the phase maps.

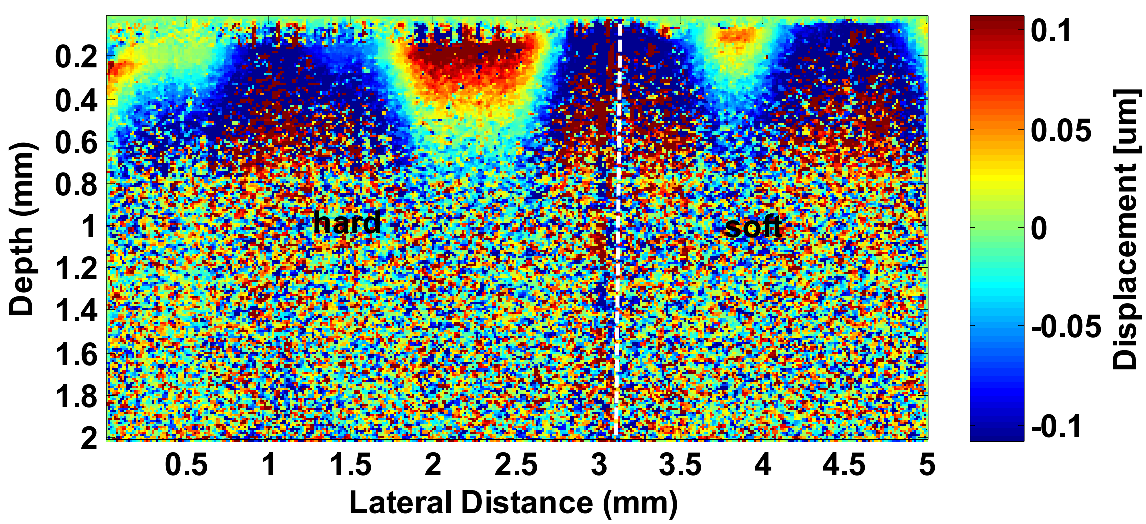

Fig. 3. Dynamic measurement of shear wave motion in the layered phantom. The color bar represents the particle displacement (in μm).

The attenuation coefficient can be estimated by measuring the damping of the shear wave as it propagates away from the ARF focal spot, as shown in Figure 4

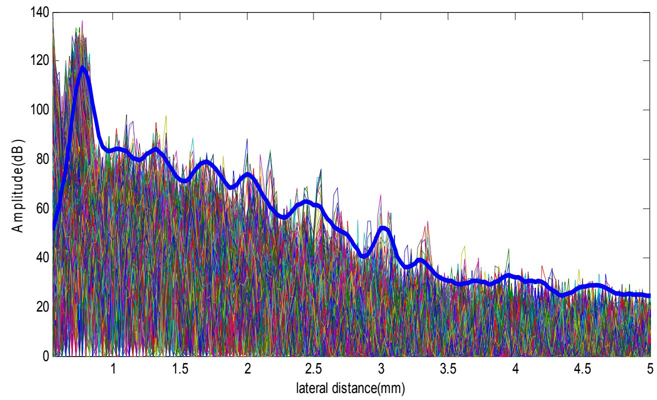

Fig. 4. The amplitude of shear wave to measure the shear wave attenuation coefficient. The blue curve is envelope of the amplitude of shear wave.

Using equation 1, the attenuation coefficient was calculated to be approximately 0.8 Np/cm. This compares favorably to previously published data on gelatin phantoms [9].

4. Discussion

OCT provides greater spatial and phase resolution than previous methods that have been used for the study of the deformation of tissue and biomaterials. This allows for the detection of small deformations in the phantoms that may be critical to the measurement of tissue mechanical properties. The spatial resolution of mechanical property maps will depend on whether reliable phase difference measurements between two locations can be made with SW-OCE. It is expected that these maps have much better spatial resolution compared to the shear wave wavelength. Since the phantom was composed of two layers with different gelatin concentrations, the measured wavelengths in these two layers of the phantom differ, as shown in Figure 3.

The OCT phase maps were acquired with a swept-source OCT (SS-OCT) system. Although SS-OCT systems typically have higher phase noise than SD-OCT systems, especially at high A-scan rates, the phase noise of the relatively low speed SS-OCT (8kHz bi-directional) used in these experiments was sufficient to measure phase changes induced by shear wave propagation. The OCT system is very sensitive as even very small vibrations or electronic device noise will effect on the phase stability. To minimize this effect, the optical table was floated using compressed air during all experiments. Future work will focus on inhomogeneous layered phantoms and more representative of vascular pathologies such as atherosclerosis and aneurysms.

5. Acknowledgments

This work is funded in part by the Canada Research Chairs program (awarded to Drs. V.X.D. Yang and M. C. Kolios), the Natural Sciences and Engineering Research Council of Canada (NSERC discovery grant 216986-2012) and the Canada Foundation for Innovation.

6. References

[1] Ophir, J., Alam, S.K., Garra, B., Kallel, F., Konofagou, E., Krouskop, T. and Varghese, T., "Elastography: ultrasonic
estimation and imaging of the elastic properties of tissues," Proc Inst Mech Eng H, 213(3), 203- 233 (1999).

[2] Sun, C., Standish, B. and Yang, V. X. D., "Optical coherence elastography: current status and future applications," Biomedical Optics, 16(4), 043001 (2011).

[3] Schmitt, J. M., "OCT elastography: imaging microscopic deformation and strain of tissue," Opt. Express, 3(6), 199-211 (1998).

[4] Liang, X., Orescanin, M., Toohey, K. S., Insana, M.F. Boppart1, S. A., "Acoustomotive optical coherence elastography for measuring material mechanical properties," Optics Letters, 34(19), 2894-2896 (2009).

[5] Greenleaf, J. F., Fatemi, M. and Insana, M., "Selected methods for imaging elastic properties of biological tissues,"Annu. Rev. Biomed. Eng, 5 ,57-78 (2003).

[6] Palmeri, M. L., McAleavey, S. A., Fong, K. L., Trahey, G. E. and Nightingale, K. R., "Dynamic mechanical response of elastic spherical inclusions to impulsive acoustic radiation force excitation," Ultrasonics. Ferroelectrics and Frequency Control. IEEE Transactions on, 53(11), 2065-2079 (2006).

[7] Razani, M., Mariampillai, A., Sun, C., Luk ,T. W.H., Yang ,V. X..D., and Kolios, M. C., "Feasibility of optical coherence elastography measurements of shear wave propagation in homogeneous tissue equivalent phantoms" *Biomed.* Opt. Express 3(5), 972-980, 2012

[8] Adler ,D. C., Huber, R., and Fujimoto, J. G., "Phase-sensitive optical coherence tomography at up to 370,000 lines per second using buffered Fourier domain mode-locked lasers" optical letter , 32(6) (2007).

[9] Urban, M. W and Greenleaf ,J.F., "Kramers-Kronig based quality factor for shear wave propagation in soft tissue,",Phys Med Biol, 54(19): 5919–5933(2009).